Geophysical Journal International

Noise-based Ballistic Wave Passive Seismic Monitoring – Part 1: Body-waves

Journal:	*Geophysical Journal International*
Manuscript ID	GJI-18-1026.R1
Manuscript Type:	Research Paper
Date Submitted by the Author:	17-Apr-2019
Complete List of Authors:	Brenguier, Florent ; Univ. Grenoble Alpes, ISTerre Courbis, Roméo; Univ. Grenoble Alpes, ISTerre; Sisprobe Mordret, Aurélien; Massachusetts Institute of Technology, Department of Earth, Atmospheric and Planetary Sciences Campman, Xander; Shell International Exploration and Production B.V. Boué, Pierre; Univ. Grenoble Alpes, ISTerre Chmiel, Małgorzata; Sisprobe; Univ. Grenoble Alpes, ISTerre Takano, Tomoya; Tohoku Univ., Solid Earth Physics Laboratory Lecocq, Thomas; Royal Observatory of Belgium, Seismology - Gravimetry Van der Veen, Wim ; Nederlandse Aardolie Maatschappij BV Postif, Sophie; Shell International Exploration and Production B.V. Hollis, Daniel; Sisprobe
Keywords:	Volcano monitoring < VOLCANOLOGY, Interferometry < GEOPHYSICAL METHODS, Seismic noise < SEISMOLOGY, Earthquake interaction, forecasting, and prediction < SEISMOLOGY, Induced seismicity < SEISMOLOGY

Noise-based Ballistic Wave Passive Seismic Monitoring – Part 1: Body-waves

F. Brenguier[1], R. Courbis[1,4], A. Mordret[2], X. Campman[3], P. Boué[1], M. Chmiel[4,1], T. Takano[5,1], T. Lecocq[6], W. Van der Veen[7], S. Postif[3], and D. Hollis[4]

[1]Institut des Sciences de la Terre, Univ. Grenoble Alpes.

[2]Massachusetts Institute of Technology.

[3]Shell.

[4]Sisprobe.

[5]Solid Earth Physics Laboratory, Tohoku Univ.

[6]Royal Observatory of Belgium

[7]Nederlandse Aardolie Maatschappij.

Corresponding author: Florent Brenguier (florent.brenguier@univ-grenoble-alpes.fr)

Université Grenoble Alpes

ISTerre

CS 40700

38058 GRENOBLE Cedex 9

FRANCE

Phone: +33 673 35 68 77

Summary

Unveiling the mechanisms of earthquake and volcanic eruption preparation requires improving our ability to monitor the rock mass response to transient stress perturbations at depth. The standard passive monitoring seismic interferometry technique based on coda-waves is robust but recovering accurate and properly localized P and S-velocity temporal anomalies at depth is intrinsically limited by the complexity of scattered, diffracted waves. In order to mitigate this limitation, we propose a complementary, novel, passive seismic monitoring approach based on detecting weak temporal changes of velocities of ballistic waves recovered from seismic noise correlations. This new technique requires dense arrays of seismic sensors in order to circumvent the bias linked to the intrinsic high sensitivity of ballistic waves recovered from noise correlations to changes in the noise source properties. In this work we use a dense network of 417 seismometers in the Groningen area of the Netherlands, one of Europe's largest gas fields. Over the course of 1 month our results show a 1.5 % apparent velocity increase of the P-wave refracted at the basement of the 700 m thick sedimentary cover. We interpret this unexpected high value of velocity increase for the refracted wave as being induced by the swings in groundwater charge and discharge in a carbonate layer with water conductive fracture networks at 700 m depth. We also observe a 0.25 % velocity decrease for the direct P-wave travelling in the near-surface sediments but conclude that it might be partially biased by changes in time in the noise source properties. The perspective of applying this new technique to detect localized continuous variations of seismic velocity perturbations at a few kilometers depth paves the way for improved in situ earthquake, volcano and producing reservoir monitoring.

Keywords: monitoring, seismic interferometry, earthquakes, volcanoes, producing reservoirs

1 Introduction

Large earthquakes and volcanic eruptions result from long-lasting, steady, pressure buildup on faults and magmatic reservoirs. However, the triggering mechanisms of impending events are thought to be initiated by short time scale stress and pore pressure transients associated with tectonic and volcanic interactions (e.g. Bouchon et al. 2011, Brenguier et al. 2014, Khoshmanesh & Shirzaei 2018) and possibly environmental perturbations (e.g. Johnson et al. 2017). Anthropogenic activities such as hydrocarbon extraction, waste-water disposal, CO_2 storage and geothermal production also induce fluid pore-pressure related deformation that can lead to the triggering of induced seismicity (Talwani 2007, Ellsworth 2013, Chang and Segall 2016). Monitoring these stress and pore-pressure perturbations continuously in time with high spatial accuracy at depth is thus critical to foresee forthcoming catastrophic tectonic and volcanic events and to improve reservoir management.

Seismic velocities are sensitive to stress and pore-pressure perturbations. This has been described in-situ for a wide range of processes like for example solid earth tides (Takano et al. 2014) and rainfall induced pore-pressure changes (Wang et al. 2017). Niu et al. (2008) used active seismic source monitoring in boreholes at 1 km depth along the San Andreas Fault and were able to observe the first clear preseismic seismic velocity-stress perturbations in the hours preceding the occurrence of nearby earthquakes. Although convincing, these observations have never been reproduced due to the costly and logistically complicated in-situ experiment.

Over the last decade, passive noise-based seismic monitoring proved success for monitoring volcanoes (Sens-Schönfelder et al. 2006, Brenguier et al. 2008a, Donaldson 2017),

earthquakes (Brenguier et al. 2008b) and environmental/climate (Lecocq et al. 2017) changes. Even though some attempts were made, no one succeeded in using passive seismic monitoring to observe clear preseismic anomalies similar to those described by Niu et al. (2008). The standard coda-based technique suffers from shortcomings that limit our ability to detect localized seismic velocity perturbations at depth. This technique also referred to as coda-wave interferometry (Poupinet et al. 1984) has the advantage of being very stable thanks to its low sensitivity to noise source property changes (Colombi et al., 2014). It thus allows detecting weak temporal changes of seismic velocities as small as 0.01 % such as those associated with solid Earth tides for example (Mao et al. 2019). However, the counterpart of this high detection capability is that the complexity of coda-wave propagation limits our ability to precisely characterize both the type (P or S) of velocity change and accurate estimates of their spatial distribution at depth.

In this work, we propose a complementary monitoring approach that uses ballistic waves reconstructed from noise correlations. This paper focuses on ballistic body-waves and the companion paper Mordret et al. 2019 focuses on using ballistic surface-waves on the same dataset with the same type of approach. Body-waves have a specific sensitivity to seismic velocity changes at depth and are potentially less affected by near-surface environmental changes than surface waves. By using ballistic waves instead of coda-waves, we can more easily model the spatial sensitivity of the temporal change observations to local velocity perturbations at depth. The drawback of using direct, ballistic body-waves instead of coda-waves is their strong sensitivity to noise source temporal variations (Colombi et al. 2014). We use dense seismic networks and azimuthal averaging to circumvent this issue but still need to carefully analyze the stability of noise sources for such type of analysis.

Different studies showed that body-wave extraction from noise correlations is possible at various scales (Roux et al. 2005, Draganov at al. 2009, Poli et al. 2012). Nakata et al. (2015) were able to implement the first passive 3-D P-wave velocity tomography from continuous ground motion recorded on a dense array of more than 2500 seismic sensors installed at Long Beach (California, USA). Recently Brenguier et al. (2016) and Nakata et al. (2016) proved the temporal stability of direct virtual body-waves between dense arrays on Piton de la Fournaise volcano thus opening the way for continuous, passive ballistic wave monitoring.

In this paper we describe the fundamental aspects of passive ballistic wave monitoring using dense arrays and further illustrate its potential by applying it to a network of 417 seismic stations in the Netherlands. We are able to measure temporal changes of apparent velocities from both direct and refracted P-waves, and thus we are able to separate the response of the near surface sediments and the basement located at 700 m depth. By providing direct observations of the rock mass response to stress changes at depth, this new passive seismic approach paves the way for improved in situ earthquake, volcano and producing reservoir monitoring.

2 Methods

The new approach is based on measuring temporal changes of apparent slowness of specific ballistic waves that have been reconstructed from noise correlations using dense arrays of seismic sensors (Boué et al., 2013b, Mordret et al. 2014, Nakata et al., 2015, Nakata et al., 2016). The underlying requirement is that, as for Nakata et al. (2015), the high number of seismic sensors (> 100) and thus of noise correlation receiver pairs allows for the reconstruction of a virtual shot-gather of sufficiently high quality to be able to isolate and measure the apparent

velocity of ballistic waves such as direct P or S-waves, refracted waves or surface waves with clear mode separation (Mordret et al. 2019).

For this purpose of properly extracting high quality ballistic waves, we gather all possible noise correlations for all receiver pairs from a dense network into a single seismic panel (propagation time versus virtual source-receiver offset) thus considering a 1D velocity model for which the apparent slowness of a reconstructed ballistic wave measured at surface can be written as:

$$n = \frac{1}{V} = \frac{\Delta_x t}{\Delta x} \qquad \text{Equation 1}$$

where n is the apparent slowness and V the apparent velocity. We can estimate n as the slope of apparent arrival times t along distance x under the assumption that the apparent velocity V is uniform along distance range Δx. We are now interested in measuring a temporal change in apparent slowness $\Delta_{Ct} n$, the index Ct being for Calendar time (Fig. 1a):

$$\Delta_{Ct} n = n_{Ct2} - n_{Ct1} = \left(\frac{\Delta_x t}{\Delta x}\right)_{Ct2} - \left(\frac{\Delta_x t}{\Delta x}\right)_{Ct1} \qquad \text{Equation 2}$$

The temporal change of apparent slowness can be measured directly as the difference of slowness estimates (from a slant-stack or beam-forming analysis for example) at different calendar times (de Cacqueray et al. 2016). Here we use an approach that estimates the temporal

change of apparent slowness as the slope of the linear regression of the travel time shifts at different calendar times for each distance offset along distance Δx (Fig. 1b):

$$\Delta_{Ct} n = \frac{\Delta_x(\Delta_{Ct} t)}{\Delta x} \qquad \text{Equation 3}$$

where $\Delta_{Ct} t$ are the measurements of travel time shifts at different offsets Δx for two different calendar times and for a specific windowed ballistic wave. This approach shows the advantage of providing a direct estimate of the uncertainty of the estimated apparent slowness temporal change by assessing how the measured travel time delays $\Delta_{Ct} t$ fit a linear regression model along distance range Δx.

From equation 2, we can derive the relation linking the temporal change of apparent slowness and apparent velocity:

$$\Delta_{Ct} n = -\frac{\Delta_{Ct} V}{V^2} \qquad \text{Equation 4}$$

By multiplying the above equation by V, the apparent uniform velocity of the studied ballistic wave, this equation leads to (Fig 1c):

$$\Delta_{Ct} n \times V = \frac{\Delta_x(\Delta_{Ct} t)}{\Delta_x t} = -\frac{\Delta_{Ct} V}{V} \qquad \text{Equation 5}$$

This later equation shows that, for small velocity perturbations (<10%) we can estimate the relative temporal change of apparent velocity, $\frac{\Delta_{Ct} V}{V}$, of a given ballistic wave by estimating the value of the slope of the linear regression of $\Delta_{Ct} t$ measurements along travel time t. This

approach is sketched on Fig. 1. It applies to any kind of ballistic arrivals that can be clearly identified and isolated on a virtual source gather section. The case of direct surface waves requires mode separation and is challenging because of dispersion that leads to different velocities for different periods at which $\Delta_{Ct}t$ values are measured (Mordret et al. 2019). As suggested in Nakata et al. (2016), this approach can also be applied to noise-correlations between two distant arrays in order to monitor diving body-waves probing magmatic reservoirs, seismic faults or producing reservoirs at a few hundreds to a few kilometers depth. It is interesting to note that in this situation of two distant arrays referred to as A and B, the estimates of temporal changes of apparent velocities can be achieved using noise-correlations between arrays A and B and B and A separately, thus providing two independent estimates of temporal velocity changes. This method can also be applied using noise correlations between an individual seismic station and a distant array. In this work we apply this approach to the monitoring of a direct and a refracted wave using noise-correlations within a single array of about 8 km wide.

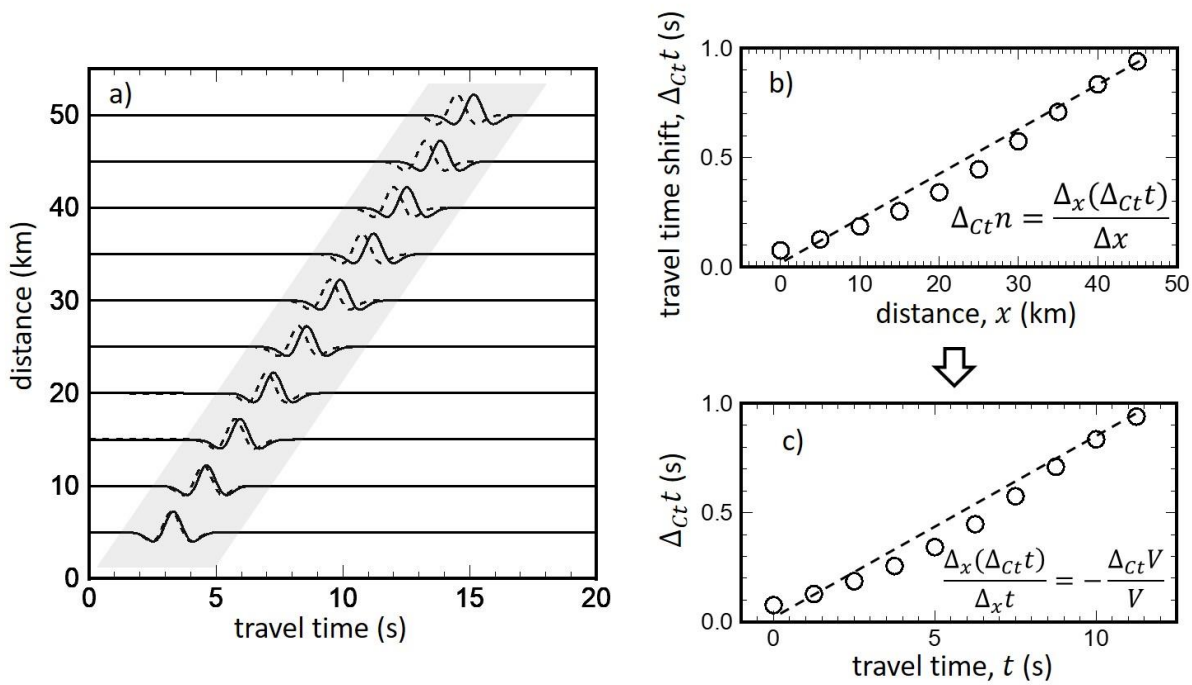

Figure 1. Procedure for ballistic-wave apparent seismic velocity monitoring. a) propagation of a direct ballistic wave. The dashed lines show the reference wave and the plain lines show the wave affected by a velocity perturbation of -7 %. b) travel time shifts measurements and linear regression along distance. c) conversion from distance to travel time by dividing distance by V, the apparent velocity of the propagating wave.

3 Data

The Groningen gas field located in the northeast of the Netherlands is one of Europe's largest natural gas field. The reservoir located at 3 km depth is thought to be 40 by 50 km wide and 250 m thick. Bourne et al. (2018) show that the gas production in this field led to a 15 MPa average reservoir pore-pressure depletion since 1995 which is associated with seismicity rates that increased as an exponential-like function.

We use a network of 417 short period seismic stations deployed in the Groningen area of the Netherlands (Fig. 2) from 11 February (day 42) to 12 March (day 71) 2017 over a time span of 30 days. The network forms a grid array with aperture of the order of 8 km and an average station distance of about 400 m.

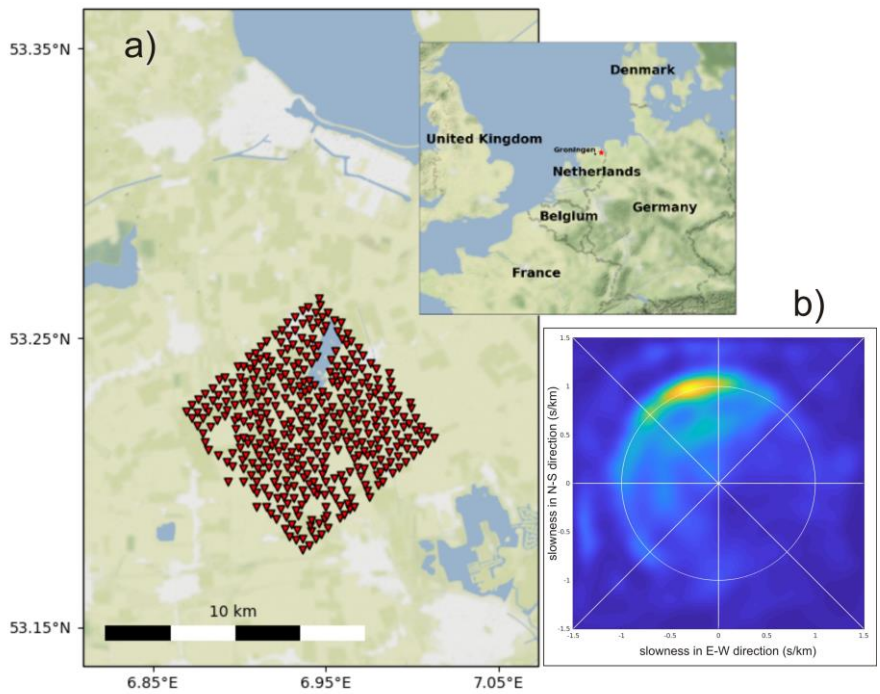

Figure 2. a) Geometry of the 417 short-period stations used in this study. b) beamforming of the 30 days of continuous seismic data in the 1-4 seconds period range.

We computed an averaged seismic section of vertical to vertical noise cross-correlations. The noise-correlations were stacked in time (over the 30 days of continuous data), in space (along distance bins of 50 meters long) and for the causal and acausal parts following Boué et al. (2013a) and Nakata et al. (2015). Figure 3 illustrates these binned data for two different

frequency ranges (1-3 Hz and 3-12 Hz). The low frequency (1-3 Hz) section mainly shows the propagation of low-velocity Rayleigh waves and also of ballistic P-waves at velocities between 1.5 and 3 km/s. The lower panel of Fig. 3 highlights the high frequency (3-12 Hz) P-waves interpreted as (1) the direct, diving P-wave with velocity of ~1700 m/s (see model on the right panel) contoured by a blue box and (2) a refracted wave at the 700 m interface with apparent velocity of ~3300 m/s contoured by a red box. Thanks to the high stability in time of the useful high-frequency ambient seismic noise, we are finally able to reconstruct repetitive in time seismic sections from the correlations of daily records of ambient seismic noise leading us to daily virtual shot seismic gathers.

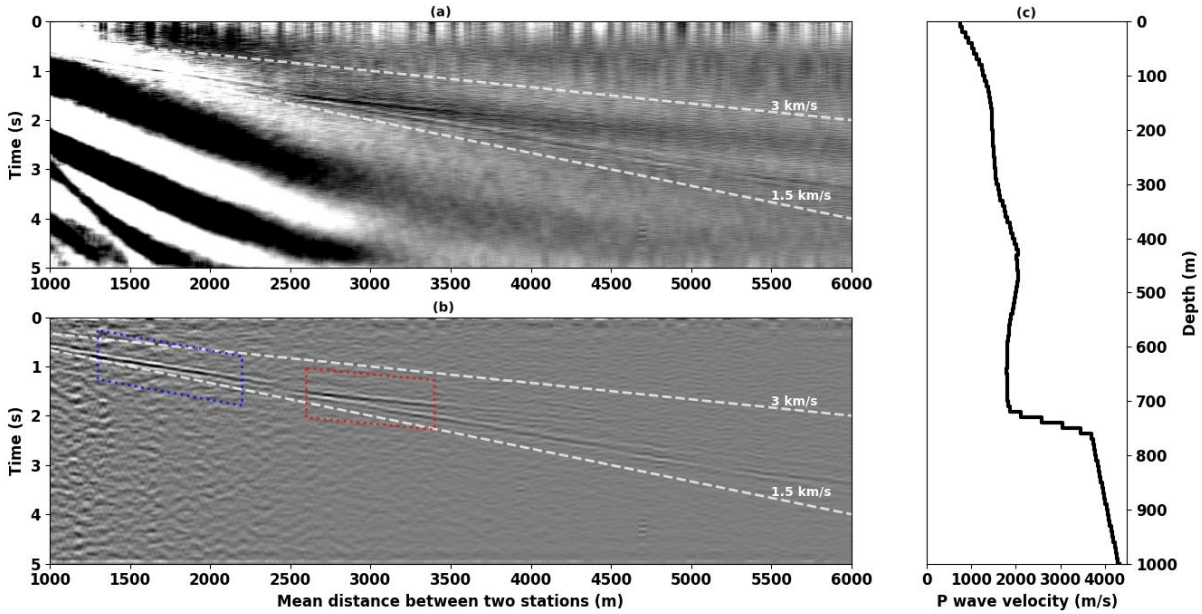

Figure 3. Noise cross-correlation averaged binned section for frequency ranges 1- 3 Hz **(a)** and 3-12 Hz **(b)**. The blue and red dashed boxes correspond to the selected windows used for the analysis for the direct and refracted waves. The right panel **(c)** illustrates the average P-wave velocity model of the area illustrating the velocities of the overburden (saturated sediments)

around 1700 m/s and of the bedrock at ~700 m depth around 3000 m/s. It has been defined using sonic logs from deep wells in the area (Kruiver et al. 2017).

4 Analysis and Results

In order to measure temporal changes, we further isolate the direct and refracted waves by applying a tapered window (Fig. 4a,b). For the time shift measurements, $\Delta_{Ct}t$, we use a cross-spectrum approach (Clarke et al. 2011) in the frequency range 3 to 8 Hz. We illustrate our approach on Figure 4 by plotting travel time shifts for the direct and refracted waves between references (stacks of days 42 to 50) and a current seismic sections (days 53 to 62 for the direct and days 48 to 57 for the refracted waves). Even though the travel time shifts measurements show large fluctuations likely associated with imperfect direct and refracted waves reconstruction and noise source changes through time, they show a clear linear trend along distance, especially for the refracted wave, indicating a clear change in apparent velocity between these two time periods. By multiplying the slope of the $\Delta_{Ct}t$ over distance linear regression by the apparent velocity of the direct (1700 m/s) and refracted (3300 m/s) waves (step b) to c) on Fig. 1), we find velocity changes of -0.25 % and +1.5% for the direct and refracted waves.

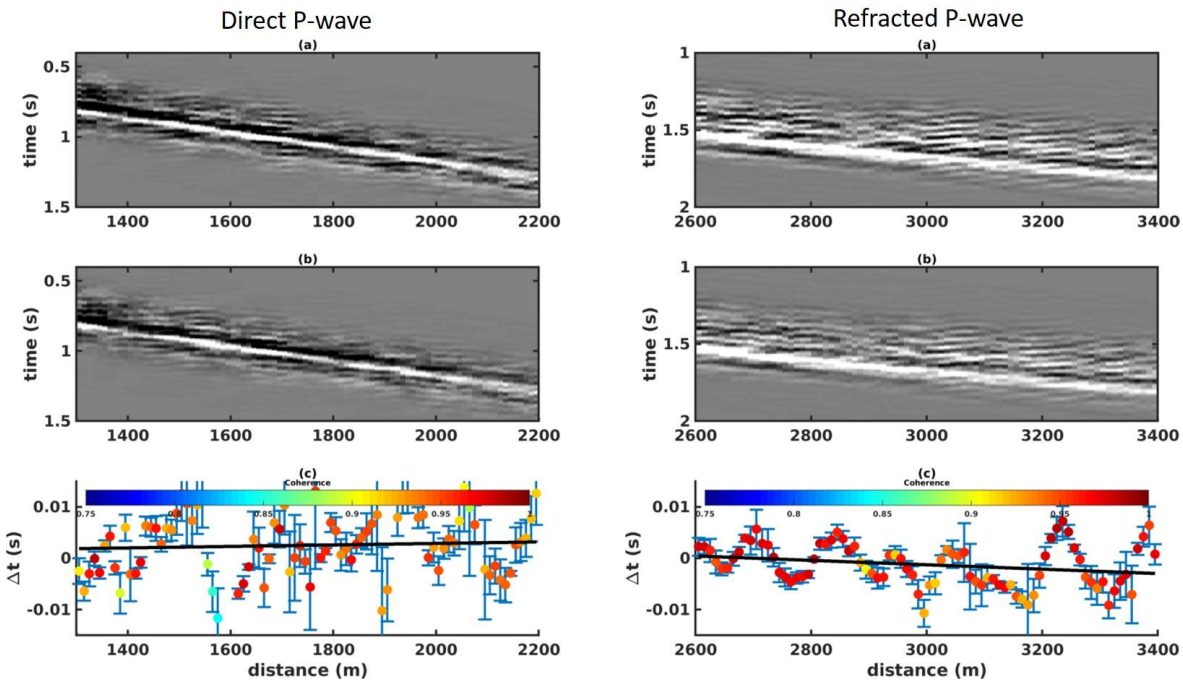

Figure 4. Travel time shifts along distance plots. **Left** a), windowed reference direct waves averaged for the time period (days 42 to 50). b) windowed current direct waves averaged for days 53 to 62. c) travel time shift measurements, $\Delta_{Ct}t$, along distance between these two direct waves. **Right** a), windowed reference refracted waves averaged for the time period (days 42 to 50). b) windowed current refracted waves averaged for days 48 to 57. c) travel time shift measurements, $\Delta_{Ct}t$, along distance between these two refracted waves.

In order to gain insights on the temporal evolution of velocity changes, we further average the daily seismic sections using a 10-days long, 1-day moving window. This leads us to 21, full 10-days averaged, daily seismic sections (from days 42 to 71). Following the method described above, we measure velocity changes ($\frac{\Delta_{Ct}V}{V}$) between each 10-days averaged seismic section and the reference section corresponding to a stack of days 42 to 50 for both the direct (Fig. 5a) and refracted (Fig. 5b) waves. The apparent velocity change curves shown on Figure 5 indicate a velocity decrease of maximum -0.25 % for the direct wave and a velocity increase of maximum 1.5 % for the refracted wave. The error bars correspond to the uncertainty of the linear

regressions estimates of the travel time shifts, $\Delta_{Ct}t$, over travel time t (Fig. 1c) using a least-square approach following Brenguier et al. 2008a.

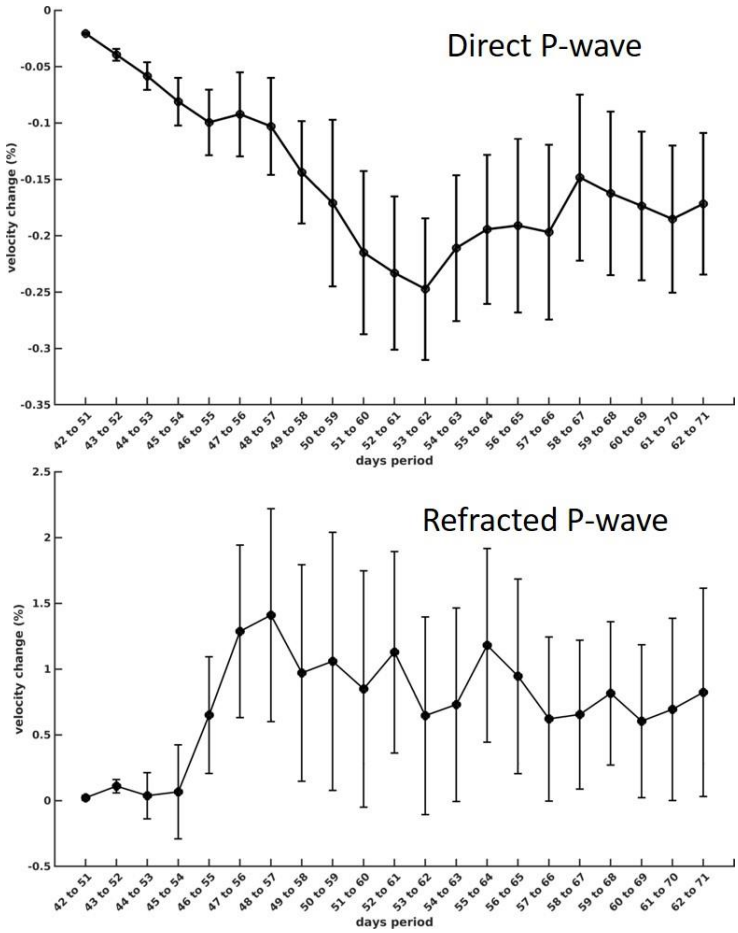

Figure 5. Apparent seismic velocity temporal changes for both the direct (top) and refracted (bottom) waves.

5 Discussions and conclusions

The most common source of error in passive, noise-based seismic monitoring results from the non-stationarity of noise sources. Furthermore, ballistic waves are much more sensitive to noise source variations than coda waves (Colombi et al. 2014). As a result, the main drawback

of this ballistic wave based monitoring method is the potential error introduced by changes in noise sources and great care has to be taken when interpreting the results. We thus need to properly assess how noise source temporal azimuthal variations can hamper our results. To do so we beamform the ambient seismic noise on a 10-days average basis in the period range 1 to 4 seconds (Fig. 2). Due to the minimum inter-station distance of 300 m we are not able to beamform the noise in the frequency range of interest (3-8 Hz) and we thus make the assumption that the 1-4 s beams are representative for the higher frequency noise characteristics. We found that the noise source distribution is strongly anisotropic with a main spot coming from the North Sea, north of our array (Fig. 2). Interestingly, the high frequency (3-8 Hz) noise correlations are quite asymmetric proving that most of the high-frequency body-waves also come from the North of our array pointing to shore break as a possible source of high-frequency noise. Our assumption of comparing the high-frequency (3-8 Hz, likely shore break) to the low-frequency (1-4 s, likely ocean microseismic) noise sources might not be fully relevant but still informative. We observe that during the time span of our analysis, the noise source distribution in the 1-4 s period range is mostly stable with small azimuthal variations of the centroid of the main spot by less than 10°. Following the theoretical predictions of travel time errors of ballistic arrival reconstructed from correlations of non-isotropically distributed noise sources from Weaver et al. (2009) and the further applications of Froment et al. (2010) and Colombi et al. (2014), we assess that, in case of a two sensors noise correlation, the error on the travel time shift measurements (Fig. 5) would lead to a velocity change uncertainty of less than 0.5 %. In our case we emphasize that our travel time shift measurements are obtained from azimuthally averaged noise correlations from the dense 417 stations array. We are thus confident that the observed velocity changes of +1.5 % for the refracted wave is mostly related to physical velocity changes.

However, the velocity decrease of 0.25 % for the direct wave might thus be partly biased by changes in the noise source properties.

In order to interpret the apparent velocity change of -0.25 % of the direct P-wave, we can consider a simple 1D model of wave propagation in the sedimentary overburden and the ray theory that predicts that the observed apparent velocity change on the direct P-wave corresponds to a real P-wave velocity perturbation averaged over the first 200 m depth (maximum distance between virtual source and stations of 2200 m). The only noticeable event during that time period is an episode of rainfall that occurred on day 53 in the region (20 mm of cumulated water height). The decrease of velocity for the direct wave could thus be related to a poro-elastic process as described by Rivet et al. (2015) and Wang et al. (2017). We will address the study of these shallow surface temporal velocity variations measurements in more details including the analysis of surface waves in a companion paper.

Following again the ray theory, the increase of apparent velocity of 1.5 % for the refracted wave can be directly attributed to a change of P-wave velocity of the carbonate bedrock at 700 m depth. Considering this hypothesis of a bedrock velocity increase, one simple interpretation could be the effect of loading from rainfall on the bedrock that would increase the confining pressure and close cracks in the bedrock. However, it is unlikely that 2 cm of additional water height on day 53, corresponding to an increase of loading of 0.2 kPa, leads to a velocity increase of 1.6 % at 700 m depth. Indeed, following Yamamura et al. (2003), and their observation of velocity-stress sensitivity of 10^{-7} Pa^{-1} the expected velocity change for a loading of 0.2 kPa should be about 0.01 %. Moreover, we checked for INSAR and GPS observations. These data don’t show any significant transient anomalies during the time span of our analysis. Finally, we also preclude the potential effects of swings in gas production in the main reservoir

at 3 km depth below our study area due to the large distance to the probed carbonate layer. These induced pressure variations are of the order of less than 0.1 MPa locally and are thus too small to potentially induce a 1.5 % velocity increase 2.3 km above in the carbonate layer. We also rule out the effects of local induced earthquakes due to the low level of seismicity during the studied time period. The most likely interpretation for this velocity increase relates to movements of fluids in water conductive fracture networks within the carbonate layer at about 700 m depth. This is discussed in a companion paper Mordret et al. 2019 that includes additional passive monitoring observations using direct surface waves.

In conclusions, even though our results are hampered by high uncertainties and are spanning a too short period to be interpreted properly, this new passive ballistic wave seismic monitoring approach has the potential for revealing seismic wave velocity temporal variations at localized areas at depth thus acting as a stress-strain probe. Even though the main drawback of this technique is that it requires dense seismic networks, we believe that this technique together with the recent step change in seismic instrumentation will lead to groundbreaking advances in our understanding of natural and induced earthquakes, volcanic eruptions and will prove useful for reservoir management.

Acknowledgments

We acknowledge two anonymous reviewers for their useful comments. This project received funding from the Shell Game Changer project HiProbe. We also acknowledge support from the French ANR grant T-ERC 2018, (FaultProbe), the European Research Council under grants no. 817803, FAULTSCAN and no. 742335, F-IMAGE and the European Union's Horizon 2020 research and innovation program under grant agreement No 776622 (PACIFIC). AM

acknowledges support from the National Science Foundation grants PLR-1643761. The data were provided by NAM (Nederlandse Aardolie Maatschappij). We acknowledge M. Campillo, N. Shapiro, G. Olivier, P. Roux, S. Garambois, R. Brossier and C. Voisin for useful discussions. The authors thank Nederlandse Aardolie Maatschappij and Shell for permission to publish.

References

Bouchon, M., Karabulut, H., Aktar, M., Özalaybey, S., Schmittbuhl, J., & Bouin, M. P. (2011). Extended nucleation of the 1999 Mw 7.6 Izmit earthquake. *science*, *331*(6019), 877-880.

Boué, P., Roux, P., Campillo, M., & de Cacqueray, B. (2013a). Double beamforming processing in a seismic prospecting context. *Geophysics*, *78*(3), V101-V108.

Boué, P., Poli, P., Campillo, M., Pedersen, H., Briand, X., & Roux, P. (2013b). Teleseismic correlations of ambient seismic noise for deep global imaging of the Earth. *Geophysical Journal International*, *194*(2), 844-848.

Bourne, S. J., Oates, S. J., & van Elk, J. (2018). The exponential rise of induced seismicity with increasing stress levels in the Groningen gas field and its implications for controlling seismic risk. *Geophysical Journal International*, *213*(3), 1693-1700.

Brenguier, F., Shapiro, N. M., Campillo, M., Ferrazzini, V., Duputel, Z., Coutant, O., & Nercessian, A. (2008a). Towards forecasting volcanic eruptions using seismic noise. *Nature Geoscience*, *1*(2), 126.

Brenguier, F., Campillo, M., Hadziioannou, C., Shapiro, N. M., Nadeau, R. M., & Larose, E. (2008b). Postseismic relaxation along the San Andreas fault at Parkfield from continuous seismological observations. Science, 321(5895), 1478-1481.

Brenguier, F., Campillo, M., Takeda, T., Aoki, Y., Shapiro, N. M., Briand, X., ... & Miyake, H. (2014). Mapping pressurized volcanic fluids from induced crustal seismic velocity drops. Science, 345(6192), 80-82.

Brenguier, F., Kowalski, P., Ackerley, N., Nakata, N., Boué, P., Campillo, M., ... & Roux, P. (2016). Toward 4D Noise-Based Seismic Probing of Volcanoes: Perspectives from a Large-N Experiment on Piton de la Fournaise Volcano. Seismological Research Letters, 87(1), 15-25.

de Cacqueray, B., Roux, P., & Campillo, M. (2016). Using slowness and azimuth fluctuations as new observables for four-dimensional reservoir seismic monitoring. *Geophysical Prospecting*, *64*(6), 1537-1555.

Chang, K. W., & Segall, P. (2016). Injection-induced seismicity on basement faults including poroelastic stressing. *Journal of Geophysical Research: Solid Earth*, *121*(4), 2708-2726.

Clarke, D., Zaccarelli, L., Shapiro, N. M., & Brenguier, F. (2011). Assessment of resolution and accuracy of the Moving Window Cross Spectral technique for monitoring crustal temporal variations using ambient seismic noise. *Geophysical Journal International*, *186*(2), 867-882.

Colombi, A., Chaput, J., Brenguier, F., Hillers, G., Roux, P., & Campillo, M. (2014). On the temporal stability of the coda of ambient noise correlations. *Comptes Rendus Geoscience*, *346*(11), 307-316.

Donaldson, C., Caudron, C., Green, R. G., Thelen, W. A., & White, R. S. (2017). Relative seismic velocity variations correlate with deformation at Kīlauea volcano. *Science advances*, *3*(6), e1700219.

Draganov, D., X. Campman, J. Thorbecke, A. Verdel, and K. Wapenaar, 2009. Reflection images from ambient seismic noise, Geophysics, 74 (5), A63–A67.

Ellsworth, W. L. (2013). Injection-induced earthquakes. *Science*, *341*(6142), 1225942.
Johnson, C. W., Fu, Y., & Bürgmann, R. (2017). Seasonal water storage, stress modulation, and California seismicity. *Science*, *356*(6343), 1161-1164.

Froment, B., Campillo, M., Roux, P., Gouedard, P., Verdel, A., & Weaver, R. L. (2010). Estimation of the effect of nonisotropically distributed energy on the apparent arrival time in correlations. *Geophysics*, 75(5), SA85-SA93.

Khoshmanesh, M., & Shirzaei, M. (2018). Episodic creep events on the San Andreas Fault caused by pore pressure variations. *Nature Geoscience*, 1.

Kruiver, P. P., van Dedem, E., Romijn, R., de Lange, G., Korff, M., Stafleu, J., ... & Doornhof, D. (2017). An integrated shear-wave velocity model for the Groningen gas field, The Netherlands. *Bulletin of Earthquake Engineering*, *15*(9), 3555-3580.

Lecocq, T., Longuevergne, L., Pedersen, H. A., Brenguier, F., & Stammler, K. (2017). Monitoring ground water storage at mesoscale using seismic noise: 30 years of continuous observation and thermo-elastic and hydrological modeling. *Scientific Reports*, *7*(1), 14241.

Mao, S., Campillo, M., van der Hilst, R. D., Brenguier, F., Stehly, L., & Hillers, G. (2019). High temporal resolution monitoring of small variations in crustal strain by dense seismic arrays. *Geophysical Research Letters*, *46*(1), 128-137.

Mordret, A., Shapiro, N. M., & Singh, S. (2014). Seismic noise-based time-lapse monitoring of the Valhall overburden. *Geophysical Research Letters*, *41*(14), 4945-4952.

Mordret, A., Courbis, R., Brenguier, F., Chmiel, M., Garambois, S., Mao, S., ... & Hollis, D. (2019). Noise-based Ballistic Wave Passive Seismic Monitoring – Part 2: Surface Waves. *Geophysical Journal International*, submitted.

Nakata, N., J. P. Chang, J. F. Lawrence, and P. Boué, (2015). Body-wave extraction and tomography at Long Beach, California, with ambient-noise tomography, J. Geophys. Res., 120, 1159–1173, doi:10.1002/2015JB01870.

Nakata, N., Boué, P., Brenguier, F., Roux, P., Ferrazzini, V., & Campillo, M. (2016). Body-and surface-wave reconstruction from seismic-noise correlations between arrays at Piton de la Fournaise volcano. Geophysical Research Letters, 43, 1047-1054.

Niu, F., Silver, P. G., Daley, T. M., Cheng, X., & Majer, E. L. (2008). Preseismic velocity changes observed from active source monitoring at the Parkfield SAFOD drill site. *Nature*, *454*(7201), 204.

Poli, P., M. Campillo, H. Pedersen, and L. W. Group, 2012. Body-wave imaging of Earth's mantle discontinuities from ambient seismic noise, Science, 338, 1063–1065.

Poupinet, G., Ellsworth, W. L., & Frechet, J. (1984). Monitoring velocity variations in the crust using earthquake doublets: An application to the Calaveras Fault, California. *Journal of Geophysical Research: Solid Earth*, *89*(B7), 5719-5731.

Rivet, D., Brenguier, F., & Cappa, F. (2015). Improved detection of preeruptive seismic velocity drops at the Piton de La Fournaise volcano. *Geophysical Research Letters*, *42*(15), 6332-6339.

Romanet, P., Bhat, H. S., Jolivet, R., & Madariaga, R. (2018). Fast and slow slip events emerge due to fault geometrical complexity. Geophysical Research Letters, 45, 4809–4819.

Rost, S., & Thomas, C. (2002). Array seismology: Methods and applications. *Reviews of geophysics*, *40*(3).

Roux, P., Sabra, K. G., Gerstoft, P., Kuperman, W. A., & Fehler, M. C. (2005). P-waves from cross-correlation of seismic noise. *Geophysical Research Letters*, *32*(19).

Sens-Schönfelder, C., & Wegler, U. (2006). Passive image interferometry and seasonal variations of seismic velocities at Merapi Volcano, Indonesia. *Geophysical research letters*, *33*(21).

Shapiro, N. M., Campillo, M., Stehly, L., & Ritzwoller, M. H. (2005). High-resolution surface-wave tomography from ambient seismic noise. *Science*, *307*(5715), 1615-1618.

Silverii, F., D'Agostino, N., Métois, M., Fiorillo, F., & Ventafridda, G. (2016). Transient deformation of karst aquifers due to seasonal and multiyear groundwater variations observed by GPS in southern Apennines (Italy). *Journal of Geophysical Research: Solid Earth*, *121*(11), 8315-8337.

Snieder, R., Grêt, A., Douma, H., & Scales, J. (2002). Coda wave interferometry for estimating nonlinear behavior in seismic velocity. *Science*, *295*(5563), 2253-2255.

Takano, T., Nishimura, T., Nakahara, H., Ohta, Y., & Tanaka, S. (2014). Seismic velocity changes caused by the Earth tide: Ambient noise correlation analyses of small-array data. *Geophysical Research Letters*, *41*(17), 6131-6136.

Talwani, P., Chen, L., & Gahalaut, K. (2007). Seismogenic permeability, ks. *Journal of Geophysical Research: Solid Earth*, *112*(B7).

Wang, Q. Y., Brenguier, F., Campillo, M., Lecointre, A., Takeda, T., & Aoki, Y. (2017). Seasonal Crustal Seismic Velocity Changes Throughout Japan. *Journal of Geophysical Research: Solid Earth*, *122*(10), 7987-8002.

Weaver, R., Froment, B., & Campillo, M. (2009). On the correlation of non-isotropically distributed ballistic scalar diffuse waves. *The Journal of the Acoustical Society of America*, 126(4), 1817-1826.

Yamamura, K., Sano, O., Utada, H., Takei, Y., Nakao, S., & Fukao, Y. (2003). Long-term observation of in situ seismic velocity and attenuation. *Journal of Geophysical Research: Solid Earth*, *108*(B6).

Noise-based Ballistic Wave Passive Seismic Monitoring – Part 1: Body-waves

F. Brenguier[1], R. Courbis[1,4], A. Mordret[2], X. Campman[3], P. Boué[1], M. Chmiel[4,1], T. Takano[5,1], T. Lecocq[6], W. Van der Veen[7], S. Postif[3], and D. Hollis[4]

[1]Institut des Sciences de la Terre, Univ. Grenoble Alpes.

[2]Massachusetts Institute of Technology.

[3]Shell.

[4]Sisprobe.

[5]Solid Earth Physics Laboratory, Tohoku Univ.

[6]Royal Observatory of Belgium

[7]Nederlandse Aardolie Maatschappij.

Corresponding author: Florent Brenguier (florent.brenguier@univ-grenoble-alpes.fr)

Université Grenoble Alpes

ISTerre

CS 40700

38058 GRENOBLE Cedex 9

FRANCE

Phone: +33 673 35 68 77

Summary

Unveiling the mechanisms of earthquake and volcanic eruption preparation requires improving our ability to monitor the rock mass response to transient stress perturbations at depth. The standard passive monitoring seismic interferometry technique based on coda-waves **is robust but recovering accurate and properly localized P and S-velocity temporal anomalies at depth is intrinsically limited by the complexity of scattered, diffracted waves**. In order to mitigate this limitation, we propose a complementary, novel, passive seismic monitoring approach based on detecting weak temporal changes of velocities of ballistic waves recovered from seismic noise correlations. This new technique requires dense arrays of seismic sensors in order to circumvent the bias linked to the intrinsic high sensitivity of ballistic waves recovered from noise correlations to changes in the noise source properties. In this work we use a dense network of 417 seismometers in the Groningen area of the Netherlands, one of Europe's largest gas fields. Over the course of 1 month our results show a 1.5 % apparent velocity increase of the P-wave refracted at the basement of the 700 m thick sedimentary cover. We interpret this unexpected high value of velocity increase for the refracted wave as being induced by the swings in groundwater charge and discharge in a carbonate layer with water conductive fracture networks at 700 m depth. We also observe a 0.25 % velocity decrease for the direct P-wave travelling in the near-surface sediments but conclude that it might be partially biased by changes in time in the noise source properties. The perspective of applying this new technique to detect localized continuous variations of seismic velocity perturbations at a few kilometers depth paves the way for improved in situ earthquake, volcano and producing reservoir monitoring.

Keywords: monitoring, seismic interferometry, earthquakes, volcanoes, producing reservoirs

1 Introduction

Large earthquakes and volcanic eruptions result from long-lasting, steady, pressure buildup on faults and magmatic reservoirs. However, the triggering mechanisms of impending events are thought to be initiated by short time scale stress and pore pressure transients associated with tectonic and volcanic interactions (e.g. Bouchon et al. 2011, Brenguier et al. 2014, Khoshmanesh & Shirzaei 2018) and possibly environmental perturbations (e.g. Johnson et al. 2017). Anthropogenic activities such as hydrocarbon extraction, waste-water disposal, CO_2 storage and geothermal production also induce fluid pore-pressure related deformation that can lead to the triggering of induced seismicity (Talwani 2007, Ellsworth 2013, Chang and Segall 2016). Monitoring these stress and pore-pressure perturbations continuously in time with high spatial accuracy at depth is thus critical to foresee forthcoming catastrophic tectonic and volcanic events and to improve reservoir management.

Seismic velocities are sensitive to stress and pore-pressure perturbations. This has been described in-situ for a wide range of processes like for example solid earth tides (Takano et al. 2014) and rainfall induced pore-pressure changes (Wang et al. 2017). Niu et al. (2008) used active seismic source monitoring in boreholes at 1 km depth along the San Andreas Fault and were able to observe the first clear preseismic seismic velocity-stress perturbations in the hours preceding the occurrence of nearby earthquakes. Although convincing, these observations have never been reproduced due to the costly and logistically complicated in-situ experiment.

Over the last decade, passive noise-based seismic monitoring proved success for monitoring volcanoes (Sens-Schönfelder et al. 2006, Brenguier et al. 2008a, Donaldson 2017),

earthquakes (Brenguier et al. 2008b) and environmental/climate (Lecocq et al. 2017) changes. Even though some attempts were made, no one succeeded in using passive seismic monitoring to observe clear preseismic anomalies similar to those described by Niu et al. (2008). The standard coda-based technique suffers from shortcomings that limit our ability to detect localized seismic velocity perturbations at depth. This technique also referred to as coda-wave interferometry (Poupinet et al. 1984) has the advantage of being very stable thanks to its low sensitivity to noise source property changes (Colombi et al., 2014). It thus allows detecting weak temporal changes of seismic velocities as small as 0.01 % such as those associated with solid Earth tides for example (Mao et al. 2019). **However, the counterpart of this high detection capability is that the complexity of coda-wave propagation limits our ability to precisely characterize both the type (P or S) of velocity change and accurate estimates of their spatial distribution at depth**.

In this work, we propose a complementary monitoring approach that uses ballistic waves reconstructed from noise correlations. **This paper focuses on ballistic body-waves and the companion paper Mordret et al. 2019 focuses on using ballistic surface-waves on the same dataset with the same type of approach.** Body-waves have a specific sensitivity to seismic velocity changes at depth and are potentially less affected by near-surface environmental changes than surface waves. By using ballistic waves instead of coda-waves, we can more easily model the spatial sensitivity of the temporal change observations to local velocity perturbations at depth. The drawback of using direct, ballistic body-waves instead of coda-waves is their strong sensitivity to noise source temporal variations (Colombi et al. 2014). We use dense seismic networks and azimuthal averaging to circumvent this issue but still need to carefully analyze the stability of noise sources for such type of analysis.

Different studies showed that body-wave extraction from noise correlations is possible at various scales (Roux et al. 2005, Draganov at al. 2009, Poli et al. 2012). Nakata et al. (2015) were able to implement the first passive 3-D P-wave velocity tomography from continuous ground motion recorded on a dense array of more than 2500 seismic sensors installed at Long Beach (California, USA). Recently Brenguier et al. (2016) and Nakata et al. (2016) proved the temporal stability of direct virtual body-waves between dense arrays on Piton de la Fournaise volcano thus opening the way for continuous, passive ballistic wave monitoring.

In this paper we describe the fundamental aspects of passive ballistic wave monitoring using dense arrays and further illustrate its potential by applying it to a network of 417 seismic stations in the Netherlands. We are able to measure temporal changes of apparent velocities from both direct and refracted P-waves, and thus we are able to separate the response of the near surface sediments and the basement located at 700 m depth. By providing direct observations of the rock mass response to stress changes at depth, this new passive seismic approach paves the way for improved in situ earthquake, volcano and producing reservoir monitoring.

2 Methods

The new approach is based on measuring temporal changes of apparent slowness of specific ballistic waves that have been reconstructed from noise correlations using dense arrays of seismic sensors (Boué et al., 2013b, Mordret et al. 2014, Nakata et al., 2015, Nakata et al., 2016). The underlying requirement is that, as for Nakata et al. (2015), the high number of seismic sensors (> 100) and thus of noise correlation receiver pairs allows for the reconstruction of a virtual shot-gather of sufficiently high quality to be able to isolate and measure the apparent

velocity of ballistic waves such as direct P or S-waves, refracted waves or surface waves with clear mode separation (Mordret et al. 2019).

For this purpose of properly extracting high quality ballistic waves, we gather all possible noise correlations for all receiver pairs from a dense network into a single seismic panel (propagation time versus virtual source-receiver offset) thus considering a 1D velocity model for which the apparent slowness of a reconstructed ballistic wave measured at surface can be written as:

$$n = \frac{1}{V} = \frac{\Delta_x t}{\Delta x} \qquad \text{Equation 1}$$

where n is the apparent slowness and V the apparent velocity. We can estimate n as the slope of apparent arrival times t along distance x under the assumption that the apparent velocity V is uniform along distance range Δx. We are now interested in measuring a temporal change in apparent slowness $\Delta_{Ct} n$, the index Ct being for Calendar time (Fig. 1a):

$$\Delta_{Ct} n = n_{Ct2} - n_{Ct1} = \left(\frac{\Delta_x t}{\Delta x}\right)_{Ct2} - \left(\frac{\Delta_x t}{\Delta x}\right)_{Ct1} \qquad \text{Equation 2}$$

The temporal change of apparent slowness can be measured directly as the difference of slowness estimates (from a slant-stack or beam-forming analysis for example) at different calendar times (de Cacqueray et al. 2016). Here we use an approach that estimates the temporal

change of apparent slowness as the slope of the linear regression of the travel time shifts at different calendar times for each distance offset along distance Δx (Fig. 1b):

$$\Delta_{Ct} n = \frac{\Delta_x(\Delta_{Ct} t)}{\Delta x} \qquad \text{Equation 3}$$

where $\Delta_{Ct} t$ are the measurements of travel time shifts at different offsets Δx for two different calendar times and for a specific windowed ballistic wave. This approach shows the advantage of providing a direct estimate of the uncertainty of the estimated apparent slowness temporal change by assessing how the measured travel time delays $\Delta_{Ct} t$ fit a linear regression model along distance range Δx.

From equation 2, we can derive the relation linking the temporal change of apparent slowness and apparent velocity:

$$\Delta_{Ct} n = -\frac{\Delta_{Ct} V}{V^2} \qquad \text{Equation 4}$$

By multiplying the above equation by V, the apparent uniform velocity of the studied ballistic wave, this equation leads to (Fig 1c):

$$\Delta_{Ct} n \times V = \frac{\Delta_x(\Delta_{Ct} t)}{\Delta_x t} = -\frac{\Delta_{Ct} V}{V} \qquad \text{Equation 5}$$

This later equation shows that, for small velocity perturbations (<10%) we can estimate the relative temporal change of apparent velocity, $\frac{\Delta_{Ct} V}{V}$, of a given ballistic wave by estimating the value of the slope of the linear regression of $\Delta_{Ct} t$ measurements along travel time t. This

approach is sketched on Fig. 1. It applies to any kind of ballistic arrivals that can be clearly identified and isolated on a virtual source gather section. The case of direct surface waves requires mode separation and is challenging because of dispersion that leads to different velocities for different periods at which $\Delta_{Ct}t$ values are measured (Mordret et al. 2019). As suggested in Nakata et al. (2016), this approach can also be applied to noise-correlations between two distant arrays in order to monitor diving body-waves probing magmatic reservoirs, seismic faults or producing reservoirs at a few hundreds to a few kilometers depth. It is interesting to note that in this situation of two distant arrays referred to as A and B, the estimates of temporal changes of apparent velocities can be achieved using noise-correlations between arrays A and B and B and A separately, thus providing two independent estimates of temporal velocity changes. This method can also be applied using noise correlations between an individual seismic station and a distant array. In this work we apply this approach to the monitoring of a direct and a refracted wave using noise-correlations within a single array of about 8 km wide.

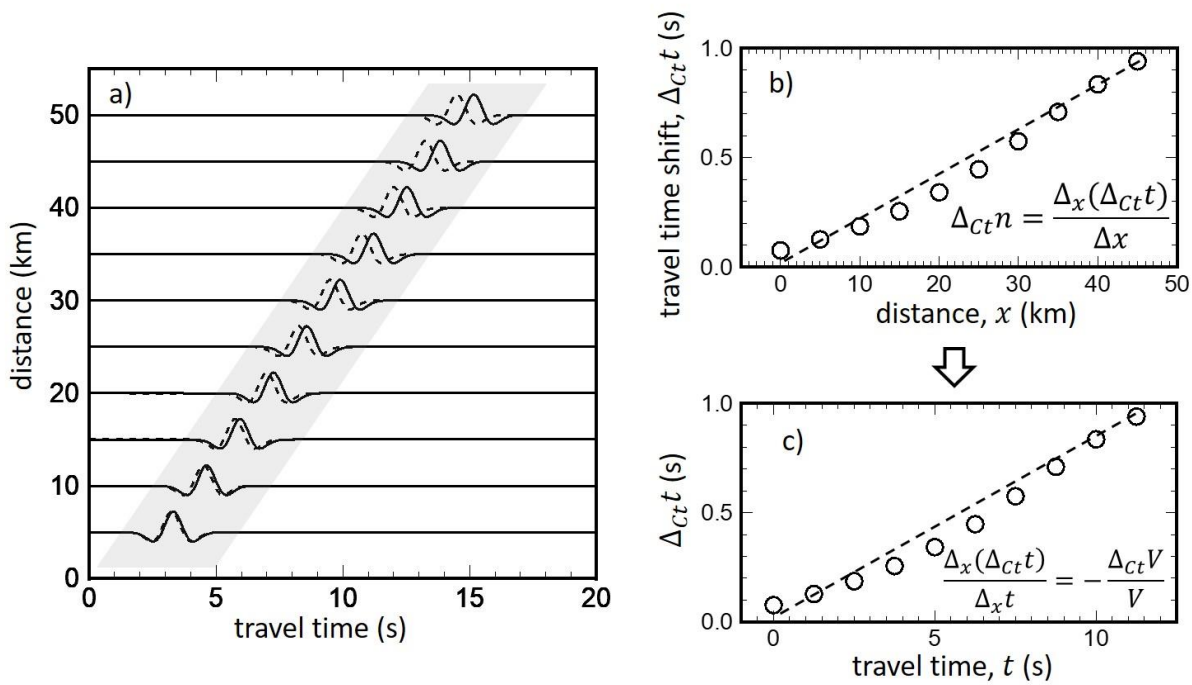

Figure 1. Procedure for ballistic-wave apparent seismic velocity monitoring. a) propagation of a direct ballistic wave. The dashed lines show the reference wave and the plain lines show the wave affected by a velocity perturbation of -7 %. b) travel time shifts measurements and linear regression along distance. c) conversion from distance to travel time by dividing distance by V, the apparent velocity of the propagating wave.

3 Data

The Groningen gas field located in the northeast of the Netherlands is one of Europe's largest natural gas field. The reservoir located at 3 km depth is thought to be 40 by 50 km wide and 250 m thick. Bourne et al. (2018) show that the gas production in this field led to a 15 MPa average reservoir pore-pressure depletion since 1995 which is associated with seismicity rates that increased as an exponential-like function.

We use a network of 417 short period seismic stations deployed in the Groningen area of the Netherlands (Fig. 2) from 11 February (day 42) to 12 March (day 71) 2017 over a time span of 30 days. The network forms a grid array with aperture of the order of 8 km **and an average station distance of about 400 m**.

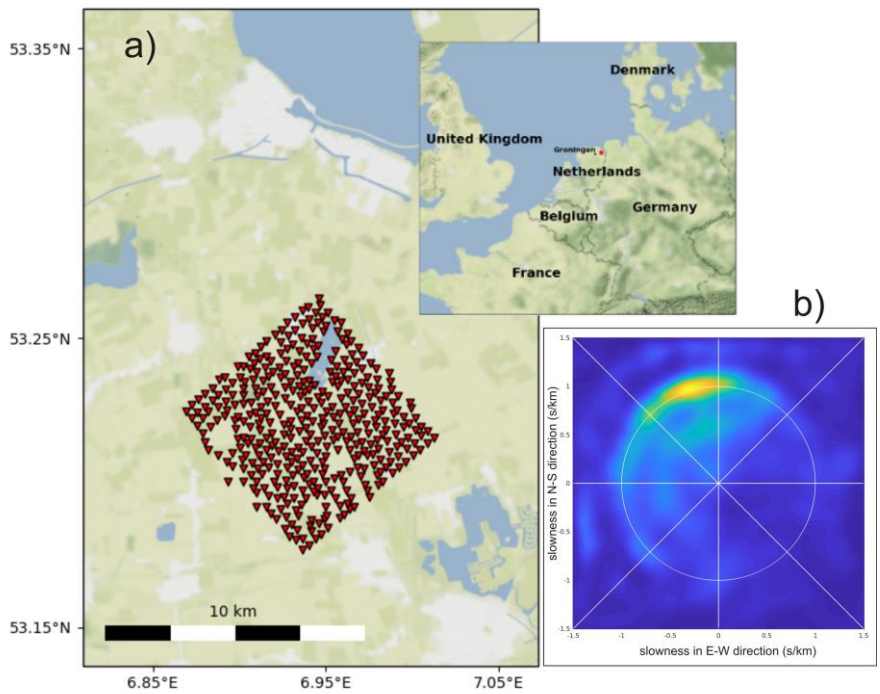

Figure 2. a) Geometry of the 417 short-period stations used in this study. b) beamforming of the 30 days of continuous seismic data in the 1-4 seconds period range.

We computed an averaged seismic section of vertical to vertical noise cross-correlations. The noise-correlations were stacked in time (over the 30 days of continuous data), in space (along distance bins of 50 meters long) and for the causal and acausal parts following Boué et al. (2013a) and Nakata et al. (2015). Figure 3 illustrates these binned data for two different

frequency ranges (1-3 Hz and 3-12 Hz). The low frequency (1-3 Hz) section mainly shows the propagation of low-velocity Rayleigh waves and also of ballistic P-waves at velocities between 1.5 and 3 km/s. The lower panel of Fig. 3 highlights the high frequency (3-12 Hz) P-waves interpreted as (1) the direct, diving P-wave with velocity of ~1700 m/s (see model on the right panel) contoured by a blue box and (2) a refracted wave at the 700 m interface with apparent velocity of ~3300 m/s contoured by a red box. Thanks to the high stability in time of the useful high-frequency ambient seismic noise, we are finally able to reconstruct repetitive in time seismic sections from the correlations of daily records of ambient seismic noise leading us to daily virtual shot seismic gathers.

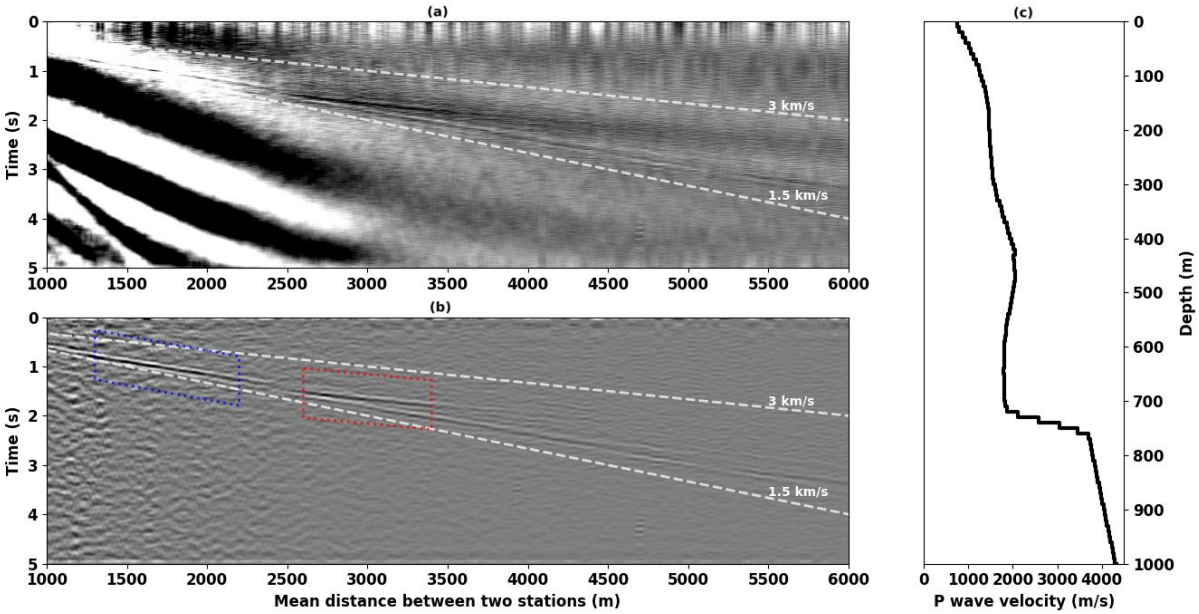

Figure 3. Noise cross-correlation averaged binned section for frequency ranges 1- 3 Hz **(a)** and 3-12 Hz **(b)**. The blue and red dashed boxes correspond to the selected windows used for the analysis for the direct and refracted waves. The right panel **(c)** illustrates the average P-wave velocity model of the area illustrating the velocities of the overburden (saturated sediments)

around 1700 m/s and of the bedrock at ~700 m depth around 3000 m/s. **It has been defined using sonic logs from deep wells in the area (Kruiver et al. 2017).**

4 Analysis and Results

In order to measure temporal changes, we further isolate the direct and refracted waves by applying a tapered window (Fig. 4a,b). For the time shift measurements, $\Delta_{Ct}t$, we use a cross-spectrum approach (Clarke et al. 2011) in the frequency range 3 to 8 Hz. We illustrate our approach on Figure 4 by plotting travel time shifts for the direct and refracted waves between references (stacks of days 42 to 50) and a current seismic sections (days 53 to 62 for the direct and days 48 to 57 for the refracted waves). Even though the travel time shifts measurements show large fluctuations **likely associated with imperfect direct and refracted waves reconstruction and noise source changes through time**, they show a clear linear trend along distance, especially for the refracted wave, indicating a clear change in apparent velocity between these two time periods. By multiplying the slope of the $\Delta_{Ct}t$ over distance linear regression by the apparent velocity of the direct (1700 m/s) and refracted (3300 m/s) waves (step b) to c) on Fig. 1), we find velocity changes of -0.25 % and +1.5% for the direct and refracted waves.

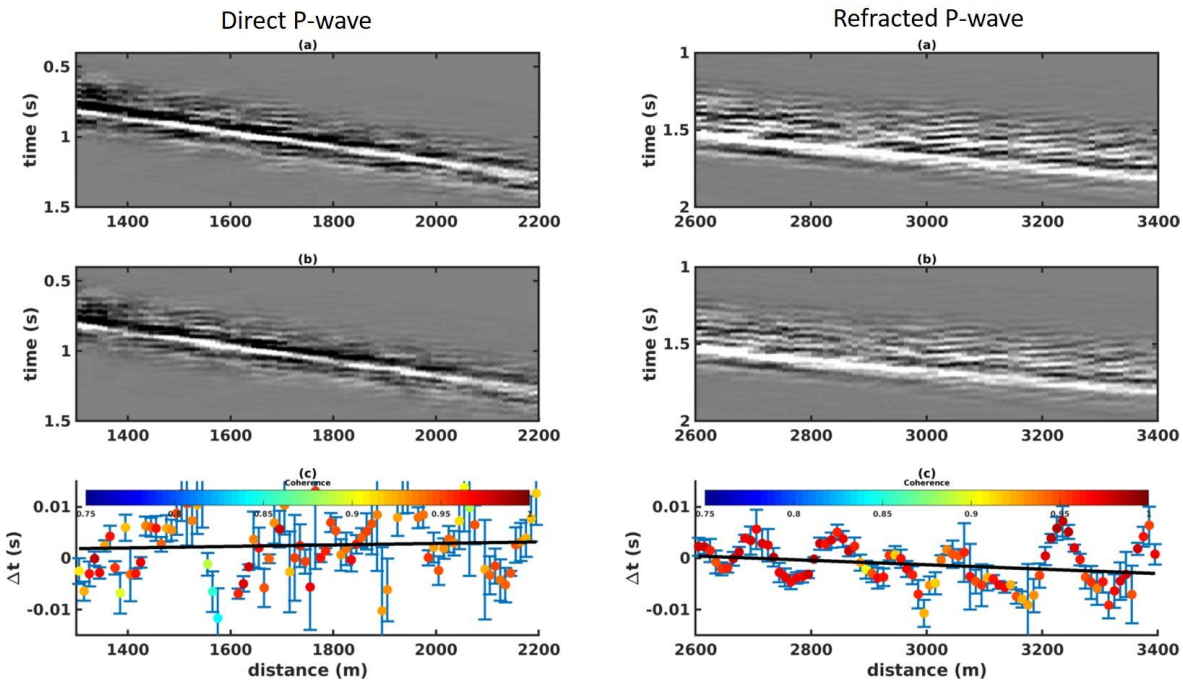

Figure 4. Travel time shifts along distance plots. **Left** a), windowed reference direct waves averaged for the time period (days 42 to 50). b) windowed current direct waves averaged for days 53 to 62. c) travel time shift measurements, $\Delta_{Ct}t$, along distance between these two direct waves. **Right** a), windowed reference refracted waves averaged for the time period (days 42 to 50). b) windowed current refracted waves averaged for days 48 to 57. c) travel time shift measurements, $\Delta_{Ct}t$, along distance between these two refracted waves.

In order to gain insights on the temporal evolution of velocity changes, we further average the daily seismic sections using a 10-days long, 1-day moving window. This leads us to 21, full 10-days averaged, daily seismic sections (from days 42 to 71). Following the method described above, we measure velocity changes ($\frac{\Delta_{Ct}V}{V}$) between each 10-days averaged seismic section and the reference section corresponding to a stack of days 42 to 50 for both the direct (Fig. 5a) and refracted (Fig. 5b) waves. The apparent velocity change curves shown on Figure 5 indicate a velocity decrease of maximum -0.25 % for the direct wave and a velocity increase of maximum 1.5 % for the refracted wave. The error bars correspond to the uncertainty of the linear

regressions estimates of the travel time shifts, $\Delta_{Ct}t$, over travel time t (Fig. 1c) using a least-square approach **following Brenguier et al. 2008a**.

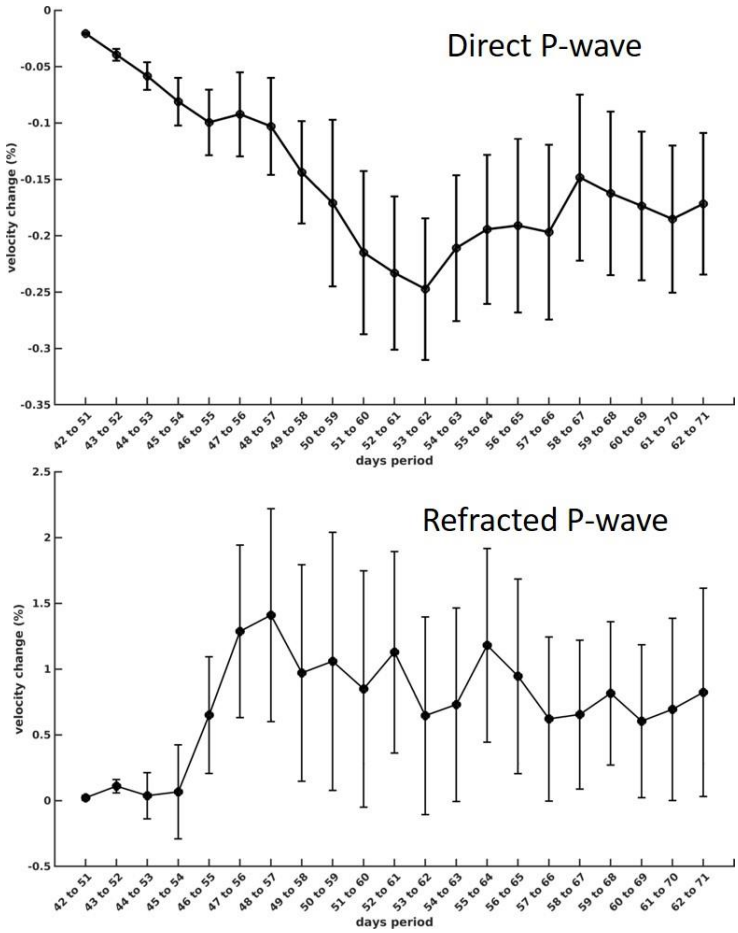

Figure 5. Apparent seismic velocity temporal changes for both the direct (top) and refracted (bottom) waves.

5 Discussions and conclusions

The most common source of error in passive, noise-based seismic monitoring results from the non-stationarity of noise sources. Furthermore, ballistic waves are much more sensitive to noise source variations than coda waves (Colombi et al. 2014). As a result, the main drawback

of this ballistic wave based monitoring method is the potential error introduced by changes in noise sources and great care has to be taken when interpreting the results. We thus need to properly assess how noise source temporal azimuthal variations can hamper our results. To do so we beamform the ambient seismic noise on a 10-days average basis in the period range 1 to 4 seconds (Fig. 2). Due to the minimum inter-station distance of 300 m we are not able to beamform the noise in the frequency range of interest (3-8 Hz) and we thus make the assumption that the 1-4 s beams are representative for the higher frequency noise characteristics. We found that the noise source distribution is strongly anisotropic with a main spot coming from the North Sea, north of our array (Fig. 2). **Interestingly, the high frequency (3-8 Hz) noise correlations are quite asymmetric proving that most of the high-frequency body-waves also come from the North of our array pointing to shore break as a possible source of high-frequency noise**. **Our assumption of comparing the high-frequency (3-8 Hz, likely shore break) to the low-frequency (1-4 s, likely ocean microseismic) noise sources might not be fully relevant but still informative**. We observe that during the time span of our analysis, the noise source distribution in the 1-4 s period range is mostly stable with small azimuthal variations of the centroid of the main spot by less than 10°. Following the theoretical predictions of travel time errors of ballistic arrival reconstructed from correlations of non-isotropically distributed noise sources from Weaver et al. (2009) and the further applications of Froment et al. (2010) and Colombi et al. (2014), we assess that, in case of a two sensors noise correlation, the error on the travel time shift measurements (Fig. 5) would lead to a velocity change uncertainty of less than 0.5 %. In our case we emphasize that our travel time shift measurements are obtained from azimuthally averaged noise correlations from the dense 417 stations array. We are thus confident that the observed velocity changes of +1.5 % for the refracted wave is mostly related to physical

velocity changes. However, the velocity decrease of 0.25 % for the direct wave might thus be partly biased by changes in the noise source properties.

In order to interpret the apparent velocity change of -0.25 % of the direct P-wave, we can consider a simple 1D model of wave propagation in the sedimentary overburden and the ray theory that predicts that the observed apparent velocity change on the direct P-wave corresponds to a real P-wave velocity perturbation averaged over the first 200 m depth (maximum distance between virtual source and stations of 2200 m). The only noticeable event during that time period is an episode of rainfall that occurred on day 53 in the region (20 mm of cumulated water height). The decrease of velocity for the direct wave could thus be related to a poro-elastic process as described by Rivet et al. (2015) and Wang et al. (2017). We will address the study of these shallow surface temporal velocity variations measurements in more details including the analysis of surface waves in a companion paper.

Following again the ray theory, the increase of apparent velocity of 1.5 % for the refracted wave can be directly attributed to a change of P-wave velocity of the carbonate bedrock at 700 m depth. Considering this hypothesis of a bedrock velocity increase, one simple interpretation could be the effect of loading from rainfall on the bedrock that would increase the confining pressure and close cracks in the bedrock. However, it is unlikely that 2 cm of additional water height on day 53, corresponding to an increase of loading of 0.2 kPa, leads to a velocity increase of 1.6 % at 700 m depth. Indeed, following Yamamura et al. (2003), and their observation of velocity-stress sensitivity of 10^{-7} Pa^{-1} the expected velocity change for a loading of 0.2 kPa should be about 0.01 %. Moreover, we checked for INSAR and GPS observations. These data don’t show any significant transient anomalies during the time span of our analysis. Finally, we also preclude the potential effects of swings in gas production in the main reservoir

at 3 km depth below our study area due to the large distance to the probed carbonate layer. These induced pressure variations are of the order of less than 0.1 MPa locally and are thus too small to potentially induce a 1.5 % velocity increase 2.3 km above in the carbonate layer. We also rule out the effects of local induced earthquakes due to the low level of seismicity during the studied time period. **The most likely interpretation for this velocity increase relates to movements of fluids in water conductive fracture networks within the carbonate layer at about 700 m depth. This is discussed in a companion paper Mordret et al. 2019 that includes additional passive monitoring observations using direct surface waves.**

In conclusions, even though our results are hampered by high uncertainties and are spanning a too short period to be interpreted properly, this new passive ballistic wave seismic monitoring approach has the potential for revealing seismic wave velocity temporal variations at localized areas at depth thus acting as a stress-strain probe. Even though the main drawback of this technique is that it requires dense seismic networks, we believe that this technique together with the recent step change in seismic instrumentation will lead to groundbreaking advances in our understanding of natural and induced earthquakes, volcanic eruptions and will prove useful for reservoir management.

Acknowledgments

We acknowledge two anonymous reviewers for their useful comments. This project received funding from the Shell Game Changer project HiProbe. We also acknowledge support from the French ANR grant T-ERC 2018, (FaultProbe), the European Research Council under grants no. 817803, FAULTSCAN and no. 742335, F-IMAGE and the European Union's Horizon 2020 research and innovation program under grant agreement No 776622 (PACIFIC). AM

acknowledges support from the National Science Foundation grants PLR-1643761. The data were provided by NAM (Nederlandse Aardolie Maatschappij). We acknowledge M. Campillo, N. Shapiro, G. Olivier, P. Roux, S. Garambois, R. Brossier and C. Voisin for useful discussions. The authors thank Nederlandse Aardolie Maatschappij and Shell for permission to publish.

References

Bouchon, M., Karabulut, H., Aktar, M., Özalaybey, S., Schmittbuhl, J., & Bouin, M. P. (2011). Extended nucleation of the 1999 Mw 7.6 Izmit earthquake. *science*, *331*(6019), 877-880.

Boué, P., Roux, P., Campillo, M., & de Cacqueray, B. (2013a). Double beamforming processing in a seismic prospecting context. *Geophysics*, *78*(3), V101-V108.

Boué, P., Poli, P., Campillo, M., Pedersen, H., Briand, X., & Roux, P. (2013b). Teleseismic correlations of ambient seismic noise for deep global imaging of the Earth. *Geophysical Journal International*, *194*(2), 844-848.

Bourne, S. J., Oates, S. J., & van Elk, J. (2018). The exponential rise of induced seismicity with increasing stress levels in the Groningen gas field and its implications for controlling seismic risk. *Geophysical Journal International*, *213*(3), 1693-1700.

Brenguier, F., Shapiro, N. M., Campillo, M., Ferrazzini, V., Duputel, Z., Coutant, O., & Nercessian, A. (2008a). Towards forecasting volcanic eruptions using seismic noise. *Nature Geoscience*, *1*(2), 126.

Brenguier, F., Campillo, M., Hadziioannou, C., Shapiro, N. M., Nadeau, R. M., & Larose, E. (2008b). Postseismic relaxation along the San Andreas fault at Parkfield from continuous seismological observations. Science, 321(5895), 1478-1481.

Brenguier, F., Campillo, M., Takeda, T., Aoki, Y., Shapiro, N. M., Briand, X., ... & Miyake, H. (2014). Mapping pressurized volcanic fluids from induced crustal seismic velocity drops. Science, 345(6192), 80-82.

Brenguier, F., Kowalski, P., Ackerley, N., Nakata, N., Boué, P., Campillo, M., ... & Roux, P. (2016). Toward 4D Noise-Based Seismic Probing of Volcanoes: Perspectives from a Large-N Experiment on Piton de la Fournaise Volcano. Seismological Research Letters, 87(1), 15-25.

de Cacqueray, B., Roux, P., & Campillo, M. (2016). Using slowness and azimuth fluctuations as new observables for four-dimensional reservoir seismic monitoring. *Geophysical Prospecting*, *64*(6), 1537-1555.

Chang, K. W., & Segall, P. (2016). Injection-induced seismicity on basement faults including poroelastic stressing. *Journal of Geophysical Research: Solid Earth*, *121*(4), 2708-2726.

Clarke, D., Zaccarelli, L., Shapiro, N. M., & Brenguier, F. (2011). Assessment of resolution and accuracy of the Moving Window Cross Spectral technique for monitoring crustal temporal variations using ambient seismic noise. *Geophysical Journal International*, *186*(2), 867-882.

Colombi, A., Chaput, J., Brenguier, F., Hillers, G., Roux, P., & Campillo, M. (2014). On the temporal stability of the coda of ambient noise correlations. *Comptes Rendus Geoscience*, *346*(11), 307-316.

Donaldson, C., Caudron, C., Green, R. G., Thelen, W. A., & White, R. S. (2017). Relative seismic velocity variations correlate with deformation at Kīlauea volcano. *Science advances*, *3*(6), e1700219.

Draganov, D., X. Campman, J. Thorbecke, A. Verdel, and K. Wapenaar, 2009. Reflection images from ambient seismic noise, Geophysics, 74 (5), A63–A67.

Ellsworth, W. L. (2013). Injection-induced earthquakes. *Science*, *341*(6142), 1225942.
Johnson, C. W., Fu, Y., & Bürgmann, R. (2017). Seasonal water storage, stress modulation, and California seismicity. *Science*, *356*(6343), 1161-1164.

Froment, B., Campillo, M., Roux, P., Gouedard, P., Verdel, A., & Weaver, R. L. (2010). Estimation of the effect of nonisotropically distributed energy on the apparent arrival time in correlations. *Geophysics*, 75(5), SA85-SA93.

Khoshmanesh, M., & Shirzaei, M. (2018). Episodic creep events on the San Andreas Fault caused by pore pressure variations. *Nature Geoscience*, 1.

Kruiver, P. P., van Dedem, E., Romijn, R., de Lange, G., Korff, M., Stafleu, J., ... & Doornhof, D. (2017). An integrated shear-wave velocity model for the Groningen gas field, The Netherlands. *Bulletin of Earthquake Engineering*, *15*(9), 3555-3580.

Lecocq, T., Longuevergne, L., Pedersen, H. A., Brenguier, F., & Stammler, K. (2017). Monitoring ground water storage at mesoscale using seismic noise: 30 years of continuous observation and thermo-elastic and hydrological modeling. *Scientific Reports*, *7*(1), 14241.

Mao, S., Campillo, M., van der Hilst, R. D., Brenguier, F., Stehly, L., & Hillers, G. (2019). High temporal resolution monitoring of small variations in crustal strain by dense seismic arrays. *Geophysical Research Letters*, *46*(1), 128-137.

Mordret, A., Shapiro, N. M., & Singh, S. (2014). Seismic noise-based time-lapse monitoring of the Valhall overburden. *Geophysical Research Letters*, *41*(14), 4945-4952.

Mordret, A., Courbis, R., Brenguier, F., Chmiel, M., Garambois, S., Mao, S., ... & Hollis, D. (2019). Noise-based Ballistic Wave Passive Seismic Monitoring – Part 2: Surface Waves. *Geophysical Journal International*, submitted.

Nakata, N., J. P. Chang, J. F. Lawrence, and P. Boué, (2015). Body-wave extraction and tomography at Long Beach, California, with ambient-noise tomography, J. Geophys. Res., 120, 1159–1173, doi:10.1002/2015JB01870.

Nakata, N., Boué, P., Brenguier, F., Roux, P., Ferrazzini, V., & Campillo, M. (2016). Body-and surface-wave reconstruction from seismic-noise correlations between arrays at Piton de la Fournaise volcano. Geophysical Research Letters, 43, 1047-1054.

Niu, F., Silver, P. G., Daley, T. M., Cheng, X., & Majer, E. L. (2008). Preseismic velocity changes observed from active source monitoring at the Parkfield SAFOD drill site. *Nature*, *454*(7201), 204.

Poli, P., M. Campillo, H. Pedersen, and L. W. Group, 2012. Body-wave imaging of Earth's mantle discontinuities from ambient seismic noise, Science, 338, 1063–1065.

Poupinet, G., Ellsworth, W. L., & Frechet, J. (1984). Monitoring velocity variations in the crust using earthquake doublets: An application to the Calaveras Fault, California. *Journal of Geophysical Research: Solid Earth*, *89*(B7), 5719-5731.

Rivet, D., Brenguier, F., & Cappa, F. (2015). Improved detection of preeruptive seismic velocity drops at the Piton de La Fournaise volcano. *Geophysical Research Letters*, *42*(15), 6332-6339.

Romanet, P., Bhat, H. S., Jolivet, R., & Madariaga, R. (2018). Fast and slow slip events emerge due to fault geometrical complexity. Geophysical Research Letters, 45, 4809–4819.

Rost, S., & Thomas, C. (2002). Array seismology: Methods and applications. *Reviews of geophysics*, *40*(3).

Roux, P., Sabra, K. G., Gerstoft, P., Kuperman, W. A., & Fehler, M. C. (2005). P-waves from cross-correlation of seismic noise. *Geophysical Research Letters*, *32*(19).

Sens-Schönfelder, C., & Wegler, U. (2006). Passive image interferometry and seasonal variations of seismic velocities at Merapi Volcano, Indonesia. *Geophysical research letters*, *33*(21).

Shapiro, N. M., Campillo, M., Stehly, L., & Ritzwoller, M. H. (2005). High-resolution surface-wave tomography from ambient seismic noise. *Science*, *307*(5715), 1615-1618.

Silverii, F., D'Agostino, N., Métois, M., Fiorillo, F., & Ventafridda, G. (2016). Transient deformation of karst aquifers due to seasonal and multiyear groundwater variations observed by GPS in southern Apennines (Italy). *Journal of Geophysical Research: Solid Earth*, *121*(11), 8315-8337.

Snieder, R., Grêt, A., Douma, H., & Scales, J. (2002). Coda wave interferometry for estimating nonlinear behavior in seismic velocity. *Science*, *295*(5563), 2253-2255.

Takano, T., Nishimura, T., Nakahara, H., Ohta, Y., & Tanaka, S. (2014). Seismic velocity changes caused by the Earth tide: Ambient noise correlation analyses of small-array data. *Geophysical Research Letters*, *41*(17), 6131-6136.

Talwani, P., Chen, L., & Gahalaut, K. (2007). Seismogenic permeability, ks. *Journal of Geophysical Research: Solid Earth*, *112*(B7).

Wang, Q. Y., Brenguier, F., Campillo, M., Lecointre, A., Takeda, T., & Aoki, Y. (2017). Seasonal Crustal Seismic Velocity Changes Throughout Japan. *Journal of Geophysical Research: Solid Earth*, *122*(10), 7987-8002.

Weaver, R., Froment, B., & Campillo, M. (2009). On the correlation of non-isotropically distributed ballistic scalar diffuse waves. *The Journal of the Acoustical Society of America*, 126(4), 1817-1826.

Yamamura, K., Sano, O., Utada, H., Takei, Y., Nakao, S., & Fukao, Y. (2003). Long-term observation of in situ seismic velocity and attenuation. *Journal of Geophysical Research: Solid Earth*, *108*(B6).